2025 IEEE XVII International Scientific and Technical Conference on Actual Problems of Electronic Instrument Engineering (APEIE) | 979-8-3315-5916-8/25/$31.00 ©2025 IEEE | DOI: 10.1109/APEIE66761.2025.11289407

Proceedings of the

XVII International Scientific and Technical Conference «Actual Problems of Electronic Instrument Engineering»

APEIE

APEIE25
Actual Problems of Electronic Instrument Engineering

14–16 November 2025, Russia

IEEE Catalog Number: CFP25471-ART
ISBN: 979-8-3315-5916-8

2025 IEEE XVII International Scientific and Technical Conference on Actual Problems of Electronic Instrument Engineering (APEIE) | 979-8-3315-5916-8/25/$31.00 ©2025 IEEE | DOI: 10.1109/APEIE66761.2025.11289252

IEEE Catalog Number: CFP25471-ART
ISBN: 979-8-3315-5916-8

2025 IEEE XVII International Scientific and Technical Conference on Actual Problems of Electronic Instrument Engineering (APEIE) | 979-8-3315-5916-8/25/$31.00 ©2025 IEEE | DOI: 10.1109/APEIE66761.2025.11289381

An Adaptive Workflow for Segmentation and Mesh Generation for Complex Multiphase Micro-CT Images of Hydrate-Bearing Rock Samples

Mikhail I. Fokin
Laboratory of mathematical modeling of multiphase processes in native and artificial *multiscale heterogeneous media*
Trofimuk Institute of Petroleum Geology and Geophysics, SBRAS
Novosibirsk, Russia
0000-0003-2090-7155

Daria V. Dobrolubova
Laboratory of mathematical modeling of multiphase processes in native and artificial *multiscale heterogeneous media*
Trofimuk Institute of Petroleum Geology and Geophysics, SBRAS
Novosibirsk, Russia
0000-0002-4577-7310

***Abstract*—Fast multiphase processes in methane hydrate–bearing samples present major challenges for quantitative micro-CT experiments. These difficulties arise from the complex and evolving pore structure, the low contrast between solid and pore-space phases, and the large data volumes generated during dynamic synchrotron imaging. Traditional segmentation approaches are often manual and inaccurate under these conditions, limiting their utility for both quantitative analysis and real-time experimental feedback. These challenges extend further to mesh generation for subsequent numerical simulations. Multiphase datasets contain components with highly variable morphology and volume fractions. Phases with complex geometry and low volumetric content require fine elements to be accurately resolved, while applying such refinement uniformly to all phases results in oversampling and excessively large meshes. Given the scale of modern dynamic micro-CT datasets, mesh models should provide a balance between accuracy and computational efficiency. In this work, we utilize a two-step approach for automated segmentation of synchrotron dynamic micro-CT data of methane hydrate formation in coal media. The method combines a deep-learning 3D U-Net with Gaussian mixture clustering for robust separation of multiphase components. Meshing the hydrate phase is particularly challenging, as individual clusters may occupy only 1–2 voxels. To overcome this, we apply a temporal continuity strategy: the adapted mesh obtained at time step T is used as the initial mesh for step T+1, offering a consistent framework for monitoring the evolution of sub-resolution structures. Quantitative comparisons demonstrate that our adaptive meshing strategy achieves a significant reduction in computational cost while maintaining geometric accuracy for the dominant phases, compared to traditional voxel-based approaches.**

Keywords—digital core, mesh model, ML segmentation, methane gas hydrates.

I. INTRODUCTION

X-ray micro-computed tomography (micro-CT) is a widely used technique for studying geomaterials, as it provides non-invasive three-dimensional visualization of processes occurring under controlled environmental conditions [1]. Synchrotron radiation enhances micro-CT by enabling time-resolved imaging of fast dynamic phenomena such as multiphase fluid flow in porous systems [2], rock deformation and failure [3] and gas-hydrate formation and dissociation [4], [5]. These experiments are essential for linking pore-scale processes with macroscopic properties.

Accurate segmentation of three-dimensional volumes of rocks remains one of the main challenges in micro-CT. Low image contrast and reconstruction artefacts often limit the performance of traditional algorithms such as thresholding, watershed, or clustering, forcing researchers to rely on manual procedures. Since segmentation accuracy strongly affects the reliability of computed rock properties and subsequent numerical modeling [6], the development of advanced automated methods is an important task. Deep learning, and in particular convolutional neural networks such as U-Net [7], has shown strong potential for CT imaging. However, its broader use is limited by the difficulty of producing annotated 3D datasets.

Meshing and its optimization represent a critical step in the analysis of multiphase micro-CT data. Digital rock models for simulation typically follow one of two paradigms. The first one is the pore-network model [8], which simplifies the pore space into a network of interconnected pores and throats. Although highly computationally efficient, this method sacrifices geometric detail, making it unsuitable for simulating processes where the exact morphology of phases, such as the formation and distribution of hydrates, is critical. The second common approach is the voxel-based approach, where each volume element (voxel) from the segmented CT scan is directly converted into a cubic mesh element [9]. While computationally straightforward, this method results in prohibitively large meshes and introduces a "staircase" effect on material interfaces, which are approximated as jagged, pixelated surfaces [10].

This study utilizes a two-step workflow for automated segmentation of synchrotron-based dynamic micro-CT data of methane hydrate formation in crushed coal. The dataset is particularly challenging due to the low contrast between hydrate and coal grains, phase-dependent gray-level variations, and the irregular morphology of the hydrate phase. The method integrates a 3D U-Net for segmentation of the rock matrix with Gaussian mixture clustering for separating pore phases, including NaBr brine and methane hydrate. This combined strategy improves segmentation robustness under low-contrast conditions and enables adaptive classification of variable pore-fluid compositions.

For mesh generation, we use an adaptive tetrahedral meshing strategy that produces body-fitted meshes and

conforms to the interfaces between solid, hydrate, and fluid phases. This approach removes the staircase effect typical of voxel grids. By refining the mesh only near interfaces and in regions with complex geometry, it reduces the number of elements compared to a uniform voxel mesh while retaining accuracy.

A difficulty arises when applying this method to phases that are close to the resolution limit of the scan. Hydrate agglomerates, often only 1–2 voxels in size, are especially problematic. Capturing these features would require fine refinement, which cancels the main advantage of adaptive meshing — a computationally efficient mesh with fewer elements. To address this, we test a temporal continuity approach. In this method, the adapted mesh obtained at time step T is used as the starting mesh for step T+1. This allows us to track the hydrate phase more consistently and reduces the need for extreme refinement at each step.

II. Data Description

The micro-CT datasets analyzed in this work were obtained during in-situ synchrotron experiment at the 2-BM beamline of the Advanced Photon Source [5]. An environmental cell containing crushed coal and NaBr brine was pressurized with methane gas and cooled to hydrate stability conditions (7 °C, 100 bar). The sample was scanned every 15 minutes with a parallel X-ray beam, producing sequential volumes that captured both hydrate-free and hydrate-bearing states. Each reconstructed dataset corresponded to a 180° resulted in 3D images of 612x612x900 voxels, with a voxel size of 6.9 µm.

Fig. 1 presents a series of zoomed in micro-CT slices highlighting three key stages of the in-situ experiment: the initial hydrate-free state, during hydrate formation, and the final hydrate-bearing state. The images illustrate the dynamic evolution of phase distribution within the crushed coal matrix. Initially, the pore space is fully saturated with NaBr brine. The experiment revealed that methane hydrate nucleation and growth took place mainly along the coal–brine interfaces. The final state reveals a significant volume of hydrate occupying the pore space. As can be seen, a major challenge is the low interfacial contrast between hydrate and coal grains, which makes segmentation based solely on grayscale thresholding unreliable. In addition, the hydrate exhibits a complex morphology, and some agglomerates have volumes close to the imaging resolution.

III. Segmentation and Meshing Workflow

A. Segmentation

For the segmentation of dynamic synchrotron CT data, we applied a two-step workflow that has been previously described in detail in [11]. The technique combines deep learning for identification of the solid framework with statistical clustering for the classification of pore-space phases.

At the first stage, coal grains are segmented using 3D convolutional neural networks of the U-Net family. The training dataset in this case was prepared in a semi-automatic manner by exploiting subvolumes where the grains remain immobile during the experiment, while the pore fluids change over time. This approach reduces the need for extensive manual labeling, which is often a bottleneck in supervised learning tasks.

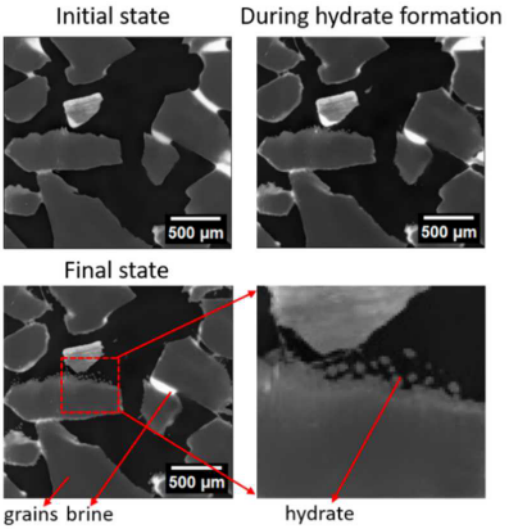

Fig. 1. Zoomed in micro-CT slices captured at different experimantal stages: initial state, during hydrate formation and after hydrate formation with describing of presented phases (coal, brine, hydrate).

At the second stage, the pore space is classified into gas, brine, and hydrate phases by applying a Gaussian mixture model (GMM) clustering algorithm. After subtracting the solid mask obtained from the U-Net, the remaining voxels are classified into several components by decomposing the mixed gray-level histogram into Gaussian distributions. Temporal consistency across sequential scans is ensured by initializing the parameters of the GMM at each time step from the values obtained at the preceding step. This approach is particularly effective in dynamic experiments where phase-contrast conditions evolve with time.

The entire segmentation pipeline was implemented in Python using TensorFlow and scikit-learn. Once the U-Net has been trained and the clustering model initialized, the workflow proceeds automatically through sequential volumes, requiring no further user intervention.

B. Algorithm for Mesh Model Generation

The initial mesh generation follows a time-independent algorithm loosely based on the principles of marching tetrahedra [12]. The process begins with the creation of a homogeneous, initial tetrahedral mesh inside the entire sample volume. This primary mesh is then adaptively refined to conform to the interfaces between material phases identified in the segmented micro-CT data.

In contrast to the classical marching tetrahedra algorithm, which explicitly reconstructs an isosurface (a triangular mesh) representing the phase boundary, our method never forms an explicit surface description. Instead, it operates directly on the volume mesh. The algorithm detects tetrahedral elements that are intersected by a phase interface by analyzing the phase labels (or "colours") assigned to the element's vertices from the segmented scan data. When such an intersection is detected, the element is locally refined by inserting new nodes and subdividing it into smaller tetrahedra.

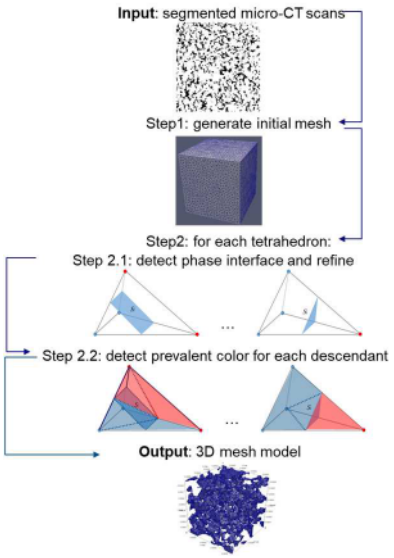

Fig. 2. Flow diagram for generating mesh model

This approach becomes particularly critical when handling the multiphase nature of hydrate-bearing rocks. While classical marching tetrahedra is straightforward for two-phase systems with only a few unique intersection patterns, the presence of three or more phases (minerals, pore space, hydrate) leads to a combinatorial explosion of possible configurations. To circumvent this complexity, we forgo the use of predefined marching tetrahedra patterns. Instead, the final phase assignment for each tetrahedron in the adapted mesh is determined by the prevalent phase among its vertices and internal integration points, as sampled from the original segmented data. This allows for a robust, automated handling of complex multiphase boundaries without explicitly cataloging every possible geometric case.

While the size of the mesh models of the samples generated using the described algorithm is significantly smaller than the voxel model size, it can become comparably large when treating the samples with small features close to the resolution limit. We cannot generally know the location of this features, unless there is an a priori information, and, therefore, have to use small-sized elements in the initial mesh.

However, since the process of hydrate formation is investigated in time, except for the first time-step, we might, in fact, possess the necessary a priori data. Based on the assumption that the physical processes of hydrate formation and evolution result in relatively small, incremental changes between scans closely spaced in time, we introduce a temporal continuity approach. In this approach, the final, adapted mesh from a previous time step T is reused as the primary mesh for the subsequent time step T+1.

The purpose of introducing this strategy is twofold. First, it leverages the geometric information already captured in the adapted mesh of time T. For features that persist between time steps—such as the mineral matrix and larger, stable hydrate structures—the mesh already possesses an optimal, refined structure. Second, we hypothesize that for small hydrate features that are poorly captured in a single scan, using the mesh from T as a prior provides a more intelligent starting point. The algorithm is not forced to "rediscover" these faint features from a coarse, homogeneous mesh at T+1 but can instead make localized adjustments to an already refined mesh that is geometrically closer to the new state. This approach aims to provide a more stable and accurate representation of the evolving hydrate volume by effectively propagating geometric constraints through time, potentially allowing the mesh to better resolve features that are at the limit of the image resolution.

IV. Experimental Results

The results of the segmentation are shown in Fig. 3, which presents zoomed in micro-CT slices and subvolumes from key stages of the experiment. The phases are clearly delineated, providing a qualitative view of the morphological evolution during hydrate formation. These segmentation results form the basis for subsequent quantitative analysis of phase volumes and for the generation of the meshes.

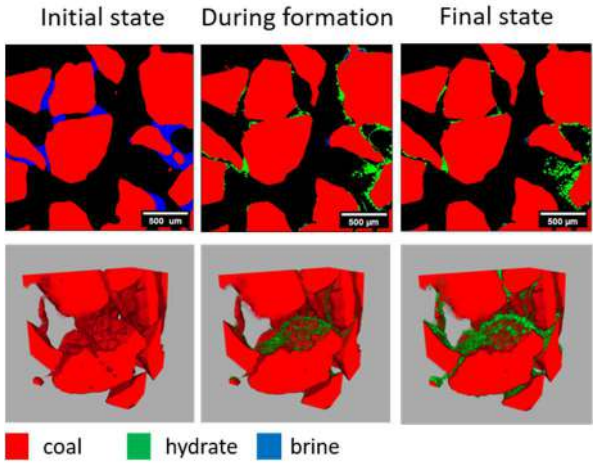

Fig. 3. The segmentation results of micro-CT data.

For the sequence of segmented scan sets in time, we compared the mesh models obtained for various initial step resolution sizes via time-independent and temporal continuity approaches. As the quality criterion for our models, we use the volume fraction of the phases of interest in the sample, i.e. grain, brine and hydrate.

A. Sensitivity to Initial Mesh Size

To establish a baseline and understand the trade-offs of our adaptive meshing algorithm, we first investigate its sensitivity to the size of the initial mesh. We consider the scan set obtained at the beginning of the process, where no hydrate formation detectable in micro-CT is formed in the sample yet. The table 1 shows the error between the phase volume fraction computed based on voxel description and the phase volume fractions, as described by the mesh model, for various initial mesh element sizes.

TABLE I. Volume Fractions of Phases of Interest According to Mesh Models with Varying Initial Mesh Step Size

Mesh step size (notional units)	N, elements	Coal		Brine	
		Volume fraction, %	error	Volume fraction, %	error
20	422 615	57.1572	4.33%	1.19263	57.68%
17.5	681 764	57.1173	4.26%	1.25004	55.64%
15	933 910	56.8082	3.70%	1.35207	52.02%
12.5	1 401 669	56.4035	2.96%	1.51501	46.24%
10	2 179 647	56.0586	2.33%	1.76412	37.40%
7.5	2 419 043	55.6376	1.56%	2.11099	25.09%
5	14 295 315	55.2483	0.85%	2.48821	11.70%
2.5	90 330 725	54.9753	0.35%	2.77716	1.45%

While the error decreases with the decrease of the initial mesh size, for the prevalent coal phase the error becomes sufficiently small (less than 5%) for even the coarsest meshes. However, for the brine, that only occupies a small part of the sample pore space, the error only reaches just above 10%, when the resulting mesh size reaches about 14 million. This foreshadows the problem of accurately capturing the hydrate agglomerates. In the following section, we only present the results for initial mesh step size of 2.5 notional units.

B. *Comparison with Voxel-Based Meshing*

To quantitatively demonstrate the advantage of our adaptive meshing strategy, we benchmarked it against the standard voxel-based approach, where each segmented voxel is directly converted into a cubic element [9]. The results of this comparison for the initial time-step are summarized in Table II.

TABLE II. COMPARISON OF MESH MODELS: ADAPTIVE VS. VOXEL-BASED

Meshing Approach	N, elements	Coal Phase Error	Brine Phase Error
Voxel-Based Mesh	~337 million	0% (by definition)	0% (by definition)
(Temporal, h=5)	~15 million	< 5%	~10%

As evident from Table II, our adaptive method generates a mesh that is over 22 times smaller than the equivalent voxel-based mesh. This massive reduction in element count directly translates to lower computational costs for subsequent numerical simulations. This benefit is achieved while maintaining a high level of accuracy for the dominant coal phase (error < 5%) and providing a geometrically superior representation with body-fitted interfaces, eliminating the staircase artifact inherent to voxel grids. This comparison underscores the primary advantage of our approach: a favorable balance between model size and geometric accuracy for efficient simulation.

C. *Performance of the Temporal Continuity Approach*

Having established the baseline performance, we evaluated the effectiveness of the temporal continuity approach for the dynamic sequence of scans. In the Figs. 4, 5, the volume fractions of coal and hydrate phases are presented for time-independent and temporal continuous approaches with initial meshes of different size, in comparison with the volume fractions computed based on segmented images. The postfix “h=5 n.u.” on the graph legend refers to the initial mesh size in notional units (these are based on the minimal mesh resolution size in pixels, but we would not go into detail in this paper).

As coal is occupying a significant part of the sample, it is, generally well approximated by the finest mesh model generated via time-independent approach. Using the temporal continuity approach with the mesh models based on the finest initial mesh improves the quality of coal phase approximation insignificantly. In the meantime, using this approach with the initial mesh of step size 5 notional units, as referred to in table 1, results in the increased quality of approximation (less than 5% error), while the mesh model size is reduced to about 15 million elements.

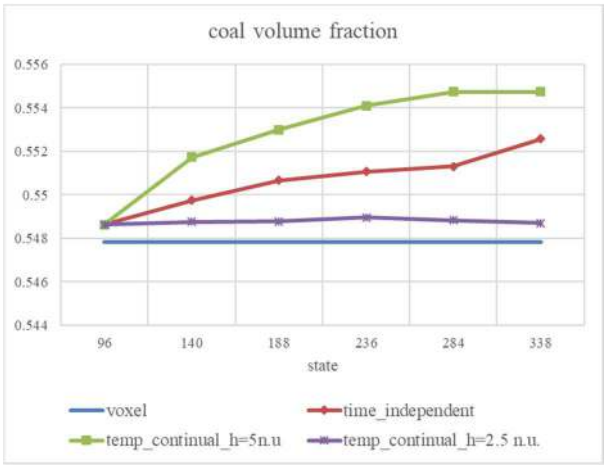

Fig. 4. Volume fraction of coal in the mesh model, for different approaches

For the hydrate phase, the method provided a limited improvement in volumetric estimation. In the Fig. 6, by visual comparison we see that the mesh model obtained via temporal continuity approach capture more small hydrate fragments, that the one obtained via time-independent approach. Nevertheless, the error of approximation for the volume fraction of hydrate formations remains above 20%. It means that while the mesh model allows for the detection of hydrate formations, it likely introduces a delay, meaning hydrates are detected later in the temporal sequence compared to their appearance in the segmented scans.

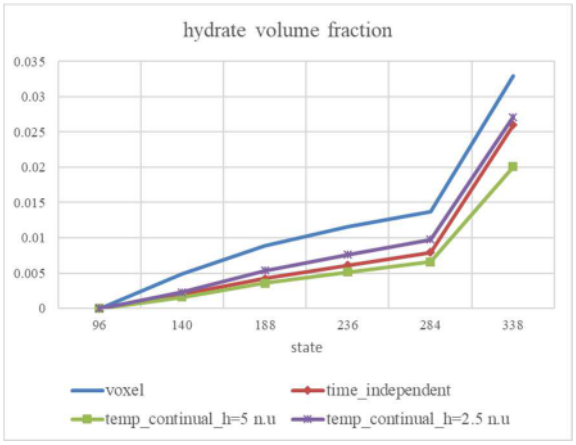

Fig. 5. Volume fraction of hydrates in the mesh model, for different approaches

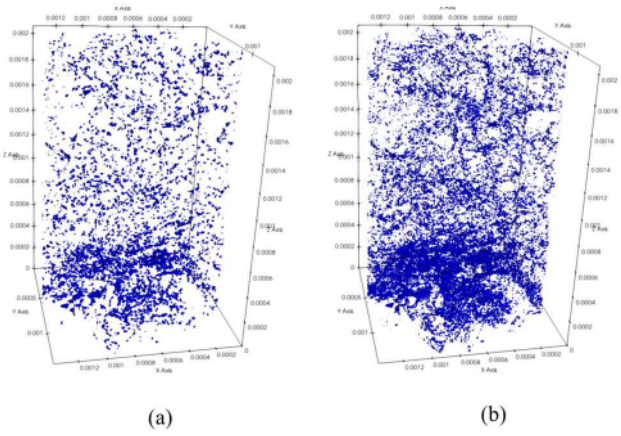

Fig. 6. Hydrate formation in the mesh model for one of the early states: (a) time-independent approach; (b) temporal continuity approach

V. Conclusion

In this work, we applied a two-step segmentation workflow to synchrotron micro-CT data of methane hydrate formation in coal. The method combines a 3D U-Net for coal matrix identification with Gaussian mixture clustering for pore-phase separation, while the training dataset is prepared in a semi-automatic way. This approach reduced the reliance on manual labelling and provided stable segmentation of the dominant coal phase across the entire time series.

The results demonstrate that our adaptive meshing workflow provides a concrete advantage over traditional methods for processing dynamic micro-CT data of hydrate-bearing rocks. The quantitative comparison with a voxel-based mesh (Table II) clearly shows that our method achieves a more than 20-fold reduction in the number of mesh elements while preserving accurate geometric representation for the dominant coal phase and eliminating staircase artifacts. As expected, the meshing results demonstrate a differential impact on the prevalent and non-prevalent phases. For the dominant coal phase, the temporal approach applied to a coarser initial mesh achieved a significant reduction in computational cost (down to 15 million elements) while maintaining high geometric accuracy (<5% error). For the non-prevalent, morphologically complex hydrate phase, the temporal continuity provided only a marginal improvement, with the volumetric error remaining above 20%. This indicates that while the method aids in computational efficiency for large, stable phases, it is insufficient to fully overcome the fundamental resolution limit for sub-pixel features. Nevertheless, the overall workflow—from semi-automatic segmentation to adaptive meshing—presents a significant step forward in managing the computational scale of dynamic micro-CT datasets, as quantitatively evidenced by the stark contrast with voxel-based meshing.

For future work, to achieve a more accurate approximation of the hydrate phase, the algorithm must be improved beyond geometric temporal propagation.

Acknowledgment

The research was supported by project No. FWZZ-2022-0030 (mesh generation) and RSF 25-71-10045 (segmentation).

References

[1] F. Fusseis, X. Xiao, C. Schrank, and F. De Carlo, “A brief guide to synchrotron radiation-based microtomography in (structural) geology and rock mechanics,” J. Struct. Geol., vol. 65, pp. 1–16, Aug. 2014, doi: 10.1016/j.jsg.2014.02.005.

[2] K. J. Dobson, S. B. Coban, S. A. McDonald, J. N. Walsh, R. C. Atwood, and P. J. Withers, “4-D imaging of sub-second dynamics in pore-scale processes using real-time synchrotron X-ray tomography,” Solid Earth, vol. 7, no. 4, pp. 1059–1073, Jul. 2016, doi: 10.5194/se-7-1059-2016.

[3] Q.-B. Zhang, K. Liu, G. Wu, and J. Zhao, “Damage and Fracture of Rocks Under Dynamic Loading,” in Handbook of Damage Mechanics: Nano to Macro Scale for Materials and Structures, 2nd ed., G. Z. Voyiadjis, Ed. Cham, Switzerland: Springer, 2022, pp. 379–422, doi: 10.1007/978-3-030-60242-0_73.

[4] V. V. Nikitin, G. A. Dugarov, A. A. Duchkov, M. I. Fokin, A. N. Drobchik, P. D. Shevchenko, F. De Carlo, and R. Mokso, “Dynamic in-situ imaging of methane hydrate formation and self-preservation in porous media,” Mar. Pet. Geol., vol. 115, p. 104234, May 2020, doi: 10.1016/j.marpetgeo.2020.104234.

[5] V. V. Nikitin, M. I. Fokin, G. A. Dugarov, A. N. Drobchik, V. De Andrade, P. D. Shevchenko, R. Mokso, and F. De Carlo, “Dynamic in situ imaging of methane hydrate formation in coal media,” Fuel, vol. 298, p. 120699, 2021, doi: 10.1016/j.fuel.2021.120699.

[6] N. Saxena, R. Hofmann, F. O. Alpak, J. Dietderich, S. Hunter, and R. J. Day-Stirrat, “Effect of image segmentation & voxel size on micro-CT computed effective transport & elastic properties,” Mar. Pet. Geol., vol. 86, pp. 972–990, Sep. 2017, doi: 10.1016/j.marpetgeo.2017.07.004.

[7] Ö. Çiçek, A. Abdulkadir, S. S. Lienkamp, T. Brox, and O. Ronneberger, “3D U-Net: Learning Dense Volumetric Segmentation from Sparse Annotation,” in Proc. MICCAI, 2016, pp. 424–432, doi: 10.1007/978-3-319-46723-8_49.

[8] Q. Xiong, T. G. Baychev, and A. P. Jivkov, “Review of pore network modelling of porous media: Experimental characterisations, network constructions and applications to reactive transport,” J. Contam. Hydrol., vol. 192, pp. 101–117, Sep. 2016, doi: 10.1016/j.jconhyd.2016.07.002.

[9] K. Koketsu, H. Fujiwara, and Y. Ikegami, “Finite-element simulation of seismic ground motion with a voxel mesh,” Pure Appl. Geophys., vol. 161, pp. 2183–2198, Nov. 2004, doi: 10.1007/s00024-004-2557-7.

[10] C. F. Berg, O. Lopez, and H. Berland, “Industrial applications of digital rock technology,” J. Pet. Sci. Eng., vol. 157, pp. 131–147, Sep. 2017, doi: 10.1016/j.petrol.2017.06.074.

[11] M. I. Fokin, V. V. Nikitin, and A. A. Duchkov, “A hybrid machine-learning approach for analysis of methane hydrate formation dynamics in porous media with synchrotron CT imaging,” J. Synchrotron Radiat., vol. 30, no. 5, pp. 978–988, Sep. 2023, doi: 10.1107/S1600577523005635.

[12] T. Lu and F. Chen, “Quantitative analysis of molecular surface based on improved marching tetrahedra algorithm,” J. Mol. Graph. Model., vol. 38, pp. 314–323, Dec. 2012, doi: 10.1016/j.jmgm.2012.07.004.